Computer-aided Simulation Model of Stator Groundwall Insulation of Induction Motor based on Current Park's Vector Approach

Amit J Modak
Research Student
Electrical Engineering
Walchand College of Engineering, Sangli

Dr. H.P. Inamdar
Professor
Electrical Engineering
Rajarambapu Institute of Technology, Sakhrale

ABSTRACT

Modeling and simulation studies published in the literature have shown that the stator winding faults are one of the major causes of induction motor failure. The spectrum analysis and AI-based fault diagnosis techniques were introduced to detect such faults at the early stage. However, there is not much mention about the deterioration of stator winding on account of degradation of stator groundwall insulation. This paper investigates the methodology to simulate the percentage of degradation related with deterioration of stator groundwall insulation of induction motor.

A design of computer based simulation model to generate the stator current data pattern for the simulation of degree of degradation of stator groundwall insulation based on Current Park's vector approach [1] is presented. The generated stator current data pattern can be further applied to any suitable artificial neural network classifier for the artificial intelligence based fault diagnosis process. The need for the evaluation, based on computer simulation is also indicated.

General Terms

Machine Intelligence, Diagnostic and Decision Supporting System

Keywords

Current Park's Transformation, induction motor, artificial intelligence (AI) techniques, Groundwall Insulation

1. INTRODUCTION

In the context of fault diagnosis based on spectrum analysis and AI-techniques, various stator winding faults were verified in the previous work [1-4]. These stator winding faults at the initial phase are in un-detected state. These faults over a period of time develop into major form to cause the sudden failure of the machine [3]. Several diagnostic media and techniques are suggested in the literature in order to diagnose stator winding faults so as to allow for carefully planned repair actions [5, 6]. The Park's Vector Approach has also been successfully applied in the diagnosis of inter-turn short circuit in stator winding [7] and air gap eccentricity [8] in three-phase induction motors. The effect of insulation degradation on account of inter-turn short circuit based on extended parks vector approach and spectrum analysis has been reported in the previous literature [3].The effect of insulation degradation due to inter-turn short circuit on stator structure and rotor bearings in the form of their vibrations has been reported in the literature [9]. The unbalance in the stator current, on account of inter-turn short circuit produces the stator vibrations. As shown in the Figure 1; the concept of the presence

of shunt resistance (R_{sh}) distributed only across the particular coil in a phase is introduced in view of inter-turn short circuit in the coil in the earlier investigation [9].
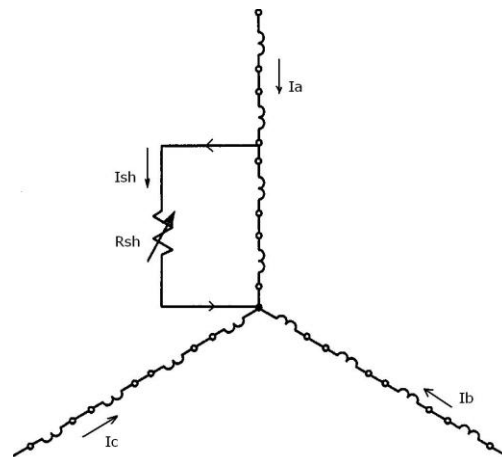

Figure 1. Stator Winding with Simulated Deterioration of Inter-turn Short Circuit

However, there is no information about the investigation in the context of degree of degradation of stator groundwall insulation. The objective of this paper is to introduce the method, which decides an extent of degradation of groundwall insulation of respective phases of stator winding. The insulation sheets between the slots and coils and on the enameled wires and between the turns in the coil are consists of different classes of insulation material. The choice depends on the maximum temperature rise permissible for each class. For each class of insulation material there exist limiting temperatures beyond which deterioration sets in and progresses rapidly. The degradation of groundwall insulation of the respective phase results in the reduction of resistance to the thermal conductivity. This results into higher heat transfer from the surface of the stator windings to the remaining part of structure. The interpretation of higher heat transfer is that the motor is subjected to extra load. Hence, motor draws more current as compared to what it would have drawn had the insulation not degraded. The increase in current is interpreted as reduction in the steady-state equivalent resistance of motor referred to stator. This is based on the interpretation of the presence of shunt resistance (R_{sh}) distributed across the entire phase as represented in the Figure 2. The degree of degradation of stator groundwall insulation is estimated on the basis of unbalance in stator phase currents.

Although there is no experimental data to indicate the time delay between inter-turn and groundwall insulation failure, it is probable that the transition between two states is not instantaneous. Therefore, like in case of inter-turn short circuit, early detection of phase short circuit during motor operation would eliminate subsequent damage to coils of the respective phase and stator core. This is useful from the point of view of repair cost and motor outage time. This leads to cost effective condition based maintenance.
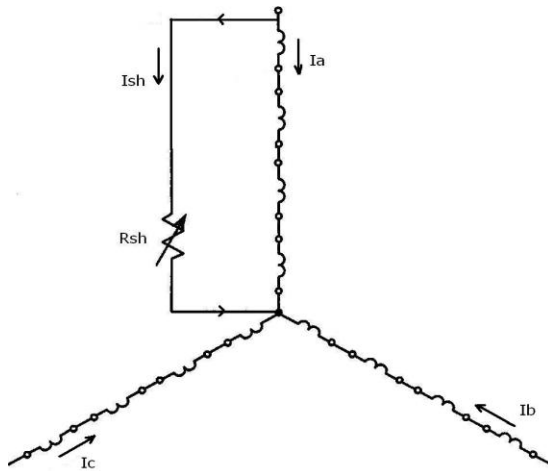

Figure 2. Stator Winding with Simulated Deterioration of Groundwall Insulation

2. FORMULATION OF WORK AND SUGGESTED APPROACH

In this investigation in view of forgoing detailed justification, a simple simulation model for the detection of degradation of stator winding groundwall insulation of cage-rotor induction motor is developed. For the induction motor of particular make, type and the frame size of suitable rating employed for particular application in an industry, it is probable that the status of degradation of stator groundwall insulation varies over considerable finite range. The finite range extends from certain minimum to permissible maximum value. The variation in the range of degradation particularly depends on several factors such as the time period over which motors are in use and the operating conditions. On experimental basis it is not feasible to collect the large set of unbalance stator current data pattern, which would model the entire range of degradation for the motor in use in particular industry. Further, in neural network based AI-technique, a large set of data pattern availability is required for the development of diagnostic model to detect the degradation of stator groundwall insulation. This is essential from the point of view of optimal design and efficient performance of the neural network classifier. Hence in this work it is decided to formulate a simulation model, which will provide the unbalanced stator current data patterns for modeling the entire range of 5% to 95 % of degradation of stator groundwall insulation.

The steps to establish aforesaid model for modeling degradation of stator groundwall insulation of cage-rotor induction motor are as under-

a) Determination of machine parameters for machine under test.

b) The computation of steady state performance of induction motor in machine variable form under minimum mechanical load condition.

c) Evaluation of maximum and minimum values of shunt resistances across the real part of equivalent steady- state motor impedance per phase referred to stator side at stator frequency under minimum mechanical load condition.

d) The computation of the numerical values of number of shunt resistances between maximum and minimum values, which are simulating different state of degradation of stator groundwall insulation.

e) Determination of various combinations of equivalent stator impedances which simulate the effect of percentage degradation of stator groundwall insulation.

f) Estimation of stator current per phase for all combinations established in step (e) as given above.

g) Development of current parks transformation model for computation of direct–axis and quadrature axis current components of three-phase stator currents with frame of reference fixed to stator.

h) Computations of parks current vector patterns for all combinations established in step (g) as given above.

i) Classification of all combinations of parks vector patterns established in step (h) as given above in accordance with the percentage of degradation of stator groundwall insulation.

The induction motor of particular make, type and the frame-size of suitable rating employed for particular application in an industry usually operate under variable load condition. In general, the motor is operating with the presence of many recipient faults, which are observable at corresponding frequencies in stator current spectrum [10-11]. These include the stator winding faults due to several causes like inter-turn short circuit etc; but other than the fault of stator groundwall insulation degradation. The fault with the stator groundwall insulation degradation would appear at supply frequency. In the spectrum the amplitude of current corresponding to supply frequency has 'two' components; one due to actual load and other due to the stator groundwall insulation degradation. In order to fetch the current component due to stator groundwall insulation degradation it is therefore essential to eliminate the current component due to load. Hence, it is obvious that the motor is to be operated at minimum mechanical load to ascertain the degree of degradation of stator groundwall insulation.

3. COMPUTER SIMULATION

Simulation analysis was conducted on three-phase; 7.5-kW, star (Y)-connected, six-pole, induction motor. The details of simulation model for the evaluation of degradation of stator winding groundwall insulation is as under-

3.1 Measurement of Induction Motor Machine Parameters

The measurement of motor parameters is based on steady-state equivalent circuit of induction motor with the rotor at stator frequency as shown in the Figure 3. The stator resistance test, no-load test and locked rotor tests were conducted to measure the following motor parameters as shown below-

R_s =Stator resistance per phase = 0.1134 Ω.

R_r =Rotor resistance per phase referred to stator = 0.6808 Ω

R_c =Core-loss resistance per phase = 235.00 Ω

X_{ls} =Stator leakage-reactance per phase = 0.16 Ω.

X_{lr} =Rotor leakage reactance per phase referred to stator = 0.16 Ω.

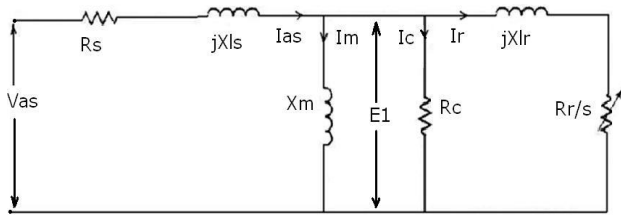X_m = Magnetizing mutual-reactance per phase = 75.00 Ω.

Figure 3. Steady-State Equivalent Circuit with Rotor at Stator Frequency

The measurement tests were performed at input power supply frequency of '50'Hz and rated operating line voltage of '415.0'volts. The stator winding is star (Y) connected with number of poles as '6'.

P = Number of poles in machine = 6

F_s = Stator input power supply line frequency = 50 Hz.

V_{ll} = Line to line stator voltage = 415Volts.

V_{as} = Stator voltage per phase = 239.60 Volts.

3.2 Performance Assessment of Motor by Steady-State Equivalent Circuit Simulation

The computer simulation of steady-state equivalent circuit of induction motor with rotor at stator frequency is done on Matlab. The measured machine parameters are used to assess the performance of cage-rotor induction motor at minimum mechanical load condition in the machine variable form. The minimum mechanical load condition is realized by decoupling the mechanical load from the shaft of motor. The operating speed of motor under minimum load condition is observed. The corresponding minimum slip value (s_nl) is used in simulation model to assess the steady state performance of motor at minimum load condition. The rotor operating speed in rpm under minimum mechanical load condition and its corresponding minimum slip value is as given in equation (1)

Nr_nl= 987.0 rpm; s_nl= 0.0133   (1)

The computations of motor variables of cage-rotor induction motor under test in machine variable form operating at minimum mechanical load are listed in Table 1.

Table 1. Induction Motor Variables in Machine Variable Form at Minimum Mechanical Load

Motor Variable	Operating Values
Zseq1_im_nl (Ω)	36.7698
Ias_nl (Amps.)	6.5162
Te_nl (N-m)	31.8675
per_eff_nl	80.7546
pf_nl	0.8705

Where, Zseq1_im_nl=Absolute value of equivalent motor-impedance per phase referred to stator at minimum mechanical load,

Ias_nl = Absolute value of stator current per phase at minimum load,

Te_nl=Air-gap/Electromagnetic torque at minimum mechanical load in N-m,

per_eff_nl= Percentage efficiency of motor at minimum mechanical load,

pf_nl= Operating power-factor of motor at minimum mechanical load.

The absolute value of stator current per phase referred from Table 1; above and as represented in equation (2) for motor operation at minimum mechanical load is the lowest observed value of balanced three-phase stator current.

Ias_nl = Absolute value of stator current per phase at minimum mechanical load = 6.5162 Amps.   (2)

This current is drawn from the balanced three-phase power supply voltage of '415.0' volts and contain fundamental line frequency component of '50'Hz only. The absence of any other frequency components confirms that the motor is healthy with very good state of stator groundwall insulation and also free from rest of the other faults. Hence, it is selected as a frame of reference to represent zero percent (0%) state of degradation of stator groundwall insulation of cage-rotor induction motor. With respect to this frame of reference, the unbalance stator current data patterns are compared to determine the percentage of degradation of stator groundwall insulation. The corresponding absolute value of stator-impedance per phase at minimum mechanical load condition based on simulation results as shown in Table 1, is given in equation (3)

Zseq1_im_nl=Absolute value of equivalent stator impedance per phase at minimum load= 36.7698Ω (3)

3.3 Computation of Motor Parameters between Minimum and Maximum Percentage of Degradation of Stator Groundwall Insulation

In most of the commercially available induction motors, coils are insulated from one another in the slots as well as in the end winding region. Therefore, the highest probability for the occurrence of inter-turn short circuit is between the turns in the same coil. Here, it is assumed that the inter-turn short circuit exists in between the two turns of the same coil. As a consequence of the inter-turn short circuit, the MMF of the phase winding in which inter-turn short circuit exists changes, as does the mutual

inductance between that phase and all other circuits in the machine. Thus, under the presence of an inter-turn short circuit, the winding function, which is MMF per unit current of the injured phase, is changed. As a consequence of such fault, self-inductance and resistance of the particular phase are changed as well as the mutual inductance between this phase and all other circuits in the machine. However, the highest probability for the occurrence of phase short circuit due to groundwall insulation degradation is in the end winding region. In this case the variation in the self -inductance of injured phase and the mutual inductance between other phases is very less as compared to the variation in the per phase resistance. Any level of percentage of degradation for particular phase is interpreted as reduction in the steady-state equivalent resistance of phase referred to stator.

It is reasonable to assume five percent (5%) reduction in real part of equivalent steady-state stator impedance per phase at minimum mechanical load as given in equation (3) to simulate some finite minimum state of degradation of stator groundwall insulation. The computation of corresponding maximum value of shunt resistance across the real part of steady-state equivalent stator impedance of motor under minimum mechanical load condition, based on computer simulation result is given as-

$$Rsh\_max = 608.1699 \ \Omega \tag{4}$$

Similarly, it is reasonable to assume ninety five percent (95%) reduction in real part of equivalent steady-state stator impedance per phase at minimum mechanical load to simulate the finite maximum state of degradation of stator groundwall insulation. The computation of corresponding minimum value of shunt resistance across the real part of steady-state equivalent stator impedance of motor under minimum mechanical load condition, based on computer simulation result is given as-

$$Rsh\_min = 1.6847 \ \Omega \tag{5}$$

Forgoing results focus the range of maximum to minimum shunt resistances, which simulate the minimum to maximum percentage degradation of stator groundwall insulation. This range is sub-divided into large number of samples to simulate the partial degrees of degradation of stator groundwall insulation. The 'm' numbers of samples of specific values of shunt resistances with an equal-space interval of 5% degradation as represented in equation (6) are computed to simulate the equal-space uniform distribution of percentage degradation over the entire range from minimum finite value of 5% to maximum finite value of 95%.

$$G = [Rsh\_xd]_{1xm} = (1xm) \text{ dimension shunt resistance matrix.} \tag{6}$$

The values of motor variables, which are modeling the 'm' number of equal –space states in between the five (5%) and ninety-five (95%) percent of degradation of stator groundwall insulation, are computed in form of matrix with - (1 x m) dimension. The corresponding values of motor variables would simulate the finite range of percentage degradation of stator groundwall insulation per-phase. The simulation results of computation of motor variables like- absolute value of equivalent motor-impedance per phase referred to stator in the form of matrix-[Zseq1_im_xd]$_{1xm}$ in Ω, absolute value of stator current per phase in the form of matrix-[Ias_nl_xd]$_{1xm}$ in amps; and motor power-factor in the form of matrix-[pf_nl_xd]$_{1xm}$ at minimum mechanical load with some finite equal-space intermediate 'xd-percent' model of degradation of stator

groundwall insulation of respective phases are as shown in Table 2.

3.4 Computation of Stator Current Data Pattern Based on Park's Current Transformation Model

The park's vector pattern learning approach has been successfully applied in the fault diagnosis of ac induction motor drive [5, 6]. In this investigation, the same approach is applied for the evaluation of different state of percentage degradation of stator groundwall insulation for respective phases of stator winding of induction motor. The Current Park's transformation model herewith simplifies the mathematical model of induction motor on account of its unique property of eliminating all time varying inductances.

Table 2. Simulation Results For M=19 Number of Samples of Equal-Space Percentage Degradation of Stator Groundwall Insulation

per_xd	Rsh_xd	Zseq1_im_xd	Ias_nl_xd	pf_nl_xd
5	608.1699	35.3853	6.7712	0.8594
10	288.0805	34.0198	7.043	0.8468
15	181.384	32.6756	7.3327	0.8327
20	128.0358	31.3555	7.6414	0.8167
25	96.0268	30.0627	7.97	0.7986
30	74.6875	28.8008	8.3192	0.778
35	59.4452	27.574	8.6894	0.7545
40	48.0134	26.3873	9.0801	0.7278
45	39.122	25.2463	9.4905	0.6973
50	32.0089	24.1575	9.9182	0.6625
55	26.1891	23.1283	10.3596	0.6228
60	21.3393	22.167	10.8089	0.5776
65	17.2356	21.2827	11.258	0.5264
70	13.7181	20.4855	11.6961	0.4688
75	10.6696	19.7858	12.1097	0.4044
80	8.0022	19.1944	12.4828	0.3335
85	5.6486	18.7215	12.7981	0.2565
90	3.5565	18.3763	13.0385	0.1742
95	1.6847	18.166	13.1895	0.0881

As a function of mains phase variables (i_a, i_b, i_c) the Current Park's vector components (i_d, i_q) are-

$$\begin{cases} i_d = \sqrt{\dfrac{2}{3}} i_a - \dfrac{1}{\sqrt{6}} i_b - \dfrac{1}{\sqrt{6}} i_c \\[4mm] i_q = \dfrac{1}{\sqrt{2}} i_b - \dfrac{1}{\sqrt{2}} i_c \end{cases} \tag{7}$$

Under ideal conditions, three phase currents lead to a Current Park's vector with the following components.

$$\begin{cases} i_d = \dfrac{\sqrt{6}}{2} I \sin \varpi t \\[4mm] i_q = \dfrac{\sqrt{6}}{2} I \sin \left(\varpi t - \dfrac{\pi}{2} \right) \end{cases} \tag{8}$$

Where; I – Maximum value of the supply phase current;

ω –Supply frequency;

t – Time variable.

The percentage of degradation of stator groundwall insulation per-phase is determined on the basis of unbalance in stator phase currents. The degree of unbalance in three-phase stator current is determined with respect to healthy state viz. zero-percentage (0%) of degradation of stator groundwall insulation. The complete set of state of degradation over the range of zero-percent (0%) to some finite maximum model of ninety-five percent (95%) of degradation is determined by including the zero-percent (0%) frame of reference to the rest of the set of 'm=19' number of samples of percentage degradation (as specified in Table 2) of stator groundwall insulation for a particular phase. The simple computer program is designed to compute the number of permutation and combinations of these percentage degradation samples viz. 'm+1=20' to model '8000' number of unique combinations. Each one of these '8000' combinations are simulating the specific variation in the state of percentage degradation of stator groundwall insulation for the respective phases viz. a, b and c of stator winding of three-phase induction motor under test. The few of these combinations comprise of equivalent motor impedance per-phase referred to stator for motor operating at minimum mechanical load, which are simulating the end limit conditions of the state of percentage degradation of stator groundwall insulation of respective phases, are listed in Table 3. The motor machine variables viz. Z_a, Z_b and Z_c represents equivalent motor impedance per-phase referred to stator in ohms(Ω) for motor operating at minimum mechanical load for all the respective phases viz. a, b and c.

Ideal condition refers to zero-percent (0%) state of percentage of degradation of stator groundwall insulation of the respective phases. The associated motor variables for this state of reference are represented by the combination no.1 in Table-3. First, the respective three-phase stator currents viz. I_a, I_b and I_c in amps; are computed and then on the basis of three to two-phase transformation model its Current Park's vector pattern is determined. The Current Park's vector representation is a circular pattern centered at the origin of the coordinate-axis as illustrated by Figure 4.
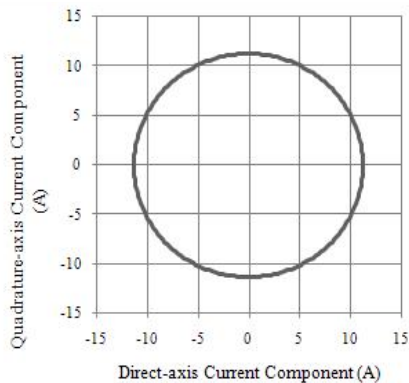

Figure 4. Reference Circular Current Park's Vector Pattern to Simulate Zero-Percent State of Degradation.

The current park's vector pattern as shown in Figure 4; is in the form of circle with radius (R) = 11.268 amps, and eccentricity (€) = 0. The circular current vector pattern with the length of major and minor axis (22.5729A.) is same as double of its radius is considered as a reference current vector pattern to represent healthy state of stator groundwall insulation of the respective phases. This reference current circular pattern contribute the phase-shift displacement of 'θ=0°' with respect to direct-axis current component vector directed along positive horizontal x-axis. It represents zero-percent state of groundwall insulation degradation in all the respective three phases.

Table 3. Combinations of Equivalent Motor Impedances to Simulate Different State of Percentage Degradation of Stator Groundwall Insulation

No.	Z_a (Ω)	Z_b (Ω)	Z_c (Ω)	Percentage of State of Degradation in Respective Phases
1	36.7698	36.7698	36.7698	Minimum-0% in all (a, b and c)
6	36.7698	36.7698	30.0627	Minimum-0% in a, b. 25% -in c.
20	36.7698	36.7698	18.166	Minimum-0% in a, b. Maximum-95% -in c.
1264	32.6756	32.6756	32.6756	15% in all (a, b, c)
101	36.7698	30.0627	36.7698	Minimum-0% in a, c. 25% -in b.
381	36.7698	18.166	36.7698	Minimum-0% in a, c. Maximum-95% -in b.
2001	30.0627	36.7698	36.7698	Minimum-0% in b, c. 25% -in a.
7601	18.166	36.7698	36.7698	Minimum-0% in b, c. Maximum-95% -in a.
43	36.7698	34.0198	34.0198	Minimum-0% in a. 10% -in b, c.
106	36.7698	30.0627	30.0627	Minimum-0% in a. 25% -in b, c.
211	36.7698	24.1575	24.1575	Minimum-0% in a. 50% -in b, c.
400	36.7698	18.166	18.166	Minimum-0% in a. Max.- 95% -in b, c.
5053	22.167	22.167	22.167	60% in all (a, b, c)
1261	32.6756	32.6756	36.7698	Minimum-0% in c. 15% -in a, b.
7981	18.166	18.166	36.7698	Minimum-0% in c. Max.- 95% -in a, b.
1605	31.3555	36.7698	31.3555	Minimum-0% in b. 20% -in a, c.
7620	18.166	36.7698	18.166	Minimum-0% in b. Max.- 95% -in a, c.
220	36.7698	24.1575	18.166	Min.-0% in a, 50%-in b, Max.-95% in c.
7611	18.166	36.7698	24.1575	Max.-95% in a, Min.- 0% in b, 50% in c.
4381	24.1575	18.166	36.7698	50% in a, Max.-95% in b, Min.-0% in c.
8000	18.166	18.166	18.166	Maximum.:95 % in all (a, b and c)

4. CLASSIFICATION OF PERCENTAGE DEGRADATION BASED ON CURRENT PARK'S VECTOR PATTERN

The computer program is designed to determine the Current Park's vector data patterns for the number of combinations of steady-state equivalent motor impedances per-phase referred to stator of respective phases as specified in Table 3. These combinations are in fact simulating the different state of percentage degradation of stator groundwall insulation of respective phases. The computer program is further designed to extract the features of Current Park's vector data pattern. The classification of various states of percentage degradation is done on the basis of comparison of extracted parameter features of various Current Park's vector data pattern with respect to the reference pattern as shown in Figure 4. The computer simulation results further implies that each one of the current park's vector data pattern is unique in representing the degree of unbalance in three-phase stator current on account of specific state of degradation of stator groundwall insulation of respective phases.

The Table 4; lists the computer simulation results, which primarily focus on the extracted parameter features like- radius (R) in amps; length of major and minor axis (M_a, M_b) in amps; phase-shift angular displacement (θ°) and eccentricity (Є) of Current Park's vector data patterns for the numbers of specific combinations listed in Table 3. The computer simulation results further provide the RMS values of three-phase balance and/or unbalance stator currents of respective phases viz. Ia, Ib and Ic in amps. The representation of the classification of various states, based on illustration of Current Park's vector data patterns is as follows-

4.1 Equal Percentage Degradation in all the Three-Phases of Stator Winding

The Current Park's vector data patterns for the simulation combination no. '1264',' 5053' and '8000' (refer Table 3 and Table 4), which is simulating '15%', '60%' and maximum of '95%' of equal state of percentage degradation in all the three respective phases viz. a, b and c is illustrated by Figure 5. The Current Park's vector data patterns are in circular form with centre at origin and of eccentricity approximately close to zero. The variation is observed with respect to reference circular current vector pattern as shown in Figure 4.
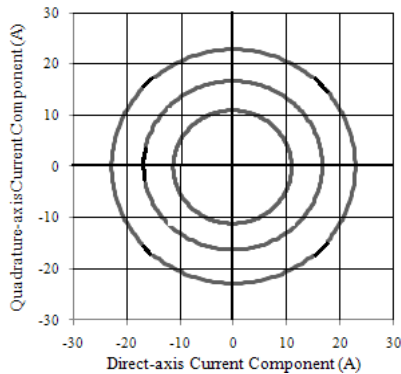

Figure 5. Current Park's Vector Pattern to Simulate Various States of Equal Percentage of Degradation in All Phases

4.2 Variation in Percentage Degradation in Phase-C from Minimum to Maximum Value and Healthy State for Phase-A and Phase-B.

The Current Park's vector data patterns for the simulation combination no. '6' and '20' (refer Table 3 and Table 4), which is simulating '25%' and maximum of '95%' of state of percentage degradation respectively in 'phase-c' and healthy state of stator groundwall insulation viz. zero-percent (0%) degradation of stator groundwall insulation for 'phase-a' and 'phase-b' is illustrated by Figure 6. The presence of some finite percentage of degradation of stator groundwall insulation in 'phase-c' introduce the change in the shape of Current Parks vector pattern from circular to elliptical form.
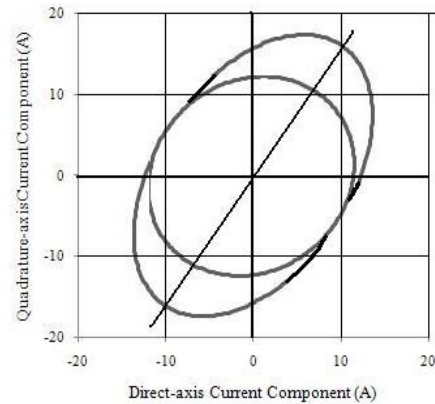

Figure 6. Current Park's Vector Pattern to Simulate 25% and Maximum 95 % of State of Degradation in Phase-C and Healthy State in Phase-A and Phase-B

4.3 Variation in Percentage Degradation in Phase-B from Minimum to Maximum Value and Healthy State for Phase-A and Phase-C

The Current Park's vector data patterns for the simulation combination no. '101' and '381' (refer Table 3 and Table 4), which is simulating '25%' and maximum of '95%' of state of percentage degradation respectively in 'phase-b' and healthy state of stator groundwall insulation for 'phase-a' and 'phase-c' is illustrated by Figure 7.
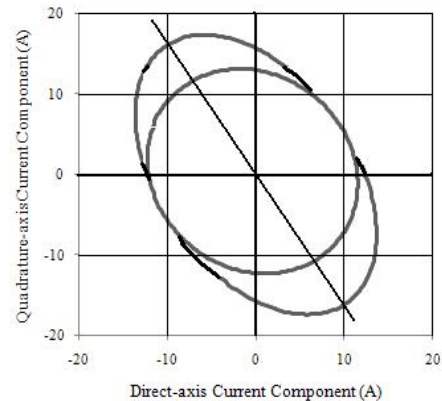

Figure 7. Current Park's Vector Pattern to Simulate 25% and Maximum 95 % of State of Degradation in Phase-B and Healthy State in Phase-A and Phase-C

4.4 Variation in Percentage Degradation in Phase-A from Minimum to Maximum Value and Healthy State for Phase-B and Phase-C.

The Current Park's vector data patterns for the simulation combination no. '2001' and '7601' (refer Table 3 and Table 4), which is simulating '25%' and maximum of '95%' of state of percentage degradation respectively in 'phase-a' and healthy state of stator groundwall insulation for 'phase-b' and 'phase-c' is illustrated by Figure 8.
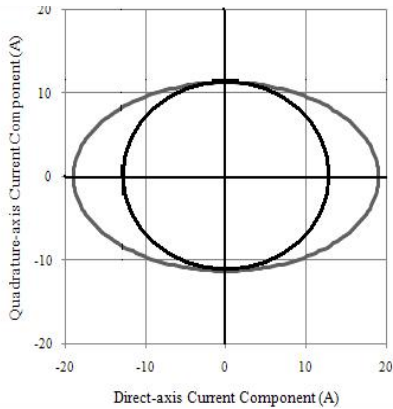

Figure 8. Current Park's Vector Pattern to Simulate 25% and Maximum 95 % of State of Degradation in Phase-A and Healthy State in Phase-B and Phase-C

4.5 Variation in Percentage Degradation in Phase-B and C from Minimum to Maximum Value and Healthy State for Phase-A.

The Current Park's vector data patterns for the simulation combination no. '43', '106', '211'and '400' (refer Table 3 and Table 4), which is simulating '10%', '25%','50%' and maximum of '95%' of state of percentage degradation respectively in 'phase-b' and 'phase-c' and healthy state of stator groundwall insulation for 'phase-a' only is illustrated by Figure 9. The deformation in an elliptical form with the variation in percentage degradation in 'phase-b' and 'phase-c' are observed with respect to reference circular current vector pattern as shown in Figure 4.
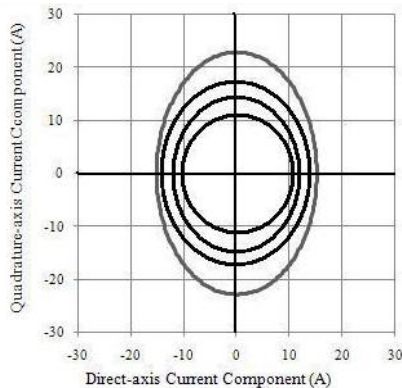

Figure 9. Current Park's Vector Pattern to Simulate 10% to 95 % Maximum State of Degradation in Phase-B and Phase-C and Healthy State of Stator Groundwall Insulation in Phase-A

4.6 Variation in Percentage Degradation in Phase-A and B from Minimum to Maximum Value and Healthy State for Phase-C.

The Current Park's vector data patterns for the simulation combination no. '1261'and '7981' (refer Table 3 and Table 4), which is simulating '15%', and maximum of '95%' of state of percentage degradation respectively in 'phase-a' and 'phase-b' and healthy state of stator groundwall insulation for 'phase-c' only is illustrated by Figure 10.

Figure 10. Current Park's Vector Pattern to Simulate 15% to 95 % Maximum State of Degradation in Phase-B and Phase-C and Healthy State of Stator Groundwall Insulation in Phase-A

4.7 Variation in Percentage Degradation in Phase-A and C from Minimum to Maximum Value and Healthy State for Phase-B.

The Current Park's vector data patterns for the simulation combination no. '1605'and '7620' (refer Table 3 and 4), which is simulating '20%', and maximum of '95%' of state of percentage degradation respectively in 'phase-a' and 'phase-c' and healthy state of stator groundwall insulation for 'phase-b' only is illustrated by Figure 11.
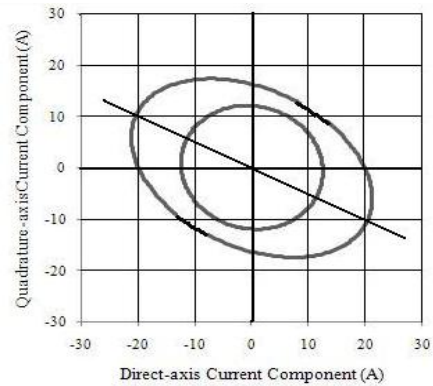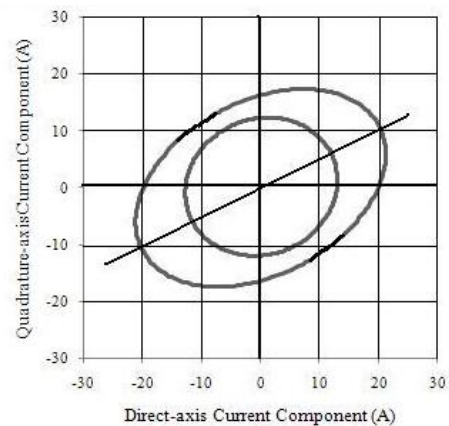

Figure 11. Current Park's Vector Pattern to Simulate 20% to 95 % Maximum State of Degradation in Phase-A and Phase-C and Healthy State of Stator Groundwall Insulation in Phase-B

Table 4. Parameter Features of Current Park's Vector Data Patterns

No.	Z_a (Ω)	Z_b (Ω)	Z_c (Ω)	I_a (A)	I_b (A)	I_c (A)	Major axis- M_a (A)	Minor axis- M_b (A)	Phase shift – (θ°)	Eccentric -city (€)	Type of Pattern
1	36.7698	36.7698	36.7698	6.5162	6.5162	6.5162	22.5729	22.5729	0	0	Circular
6	36.7698	36.7698	30.0627	6.5162	6.5162	7.97	25.9299	22.5733	59.4777	0.4921	Elliptic
20	36.7698	36.7698	18.166	6.5162	6.5162	13.1895	37.9827	22.5752	59.6434	0.8042	Elliptic
1264	32.6756	32.6756	32.6756	7.3327	7.3327	7.3327	25.4012	25.4012	0	0	Circular
101	36.7698	30.0627	36.7698	6.5162	7.97	6.5162	25.9299	22.5733	-59.4777	0.4921	Elliptic
381	36.7698	18.166	36.7698	6.5162	13.1895	6.5162	37.9827	22.5752	-59.6434	0.8042	Elliptic
2527	28.8008	28.8008	28.8008	8.3192	8.3192	8.3192	28.8187	28.8187	0	0	Circular
2001	30.0627	36.7698	36.7698	7.97	6.5162	6.5162	25.9303	22.5729	180.0	0.4921	Elliptic
7601	18.166	36.7698	36.7698	13.1895	6.5162	6.5162	37.9841	22.5729	180.0	0.8043	Elliptic
43	36.7698	34.0198	34.0198	6.5162	7.043	7.043	24.3976	23.1811	-90	0.3118	Elliptic
106	36.7698	30.0627	30.0627	6.5162	7.97	7.97	27.609	24.2516	-90	0.4779	Elliptic
211	36.7698	24.1575	24.1575	6.5162	9.9182	9.9182	34.3578	26.5012	-90	0.6364	Elliptic
400	36.7698	18.166	18.166	6.5162	13.1895	13.1895	45.6897	30.2785	-90	0.7489	Elliptic
5053	22.167	22.167	22.167	10.8089	10.8089	10.8089	37.4431	37.4431	0	0	Circular
1261	32.6756	32.6756	36.7698	7.3327	7.3327	6.5162	25.401	23.5159	-30.5555	0.378	Elliptic
7981	18.166	18.166	36.7698	13.1895	13.1895	6.5162	45.6882	30.2806	-30.3976	0.7488	Elliptic
1204	32.6756	36.7698	32.6756	7.3327	6.5162	7.3327	25.401	23.5159	30.5555	0.378	Elliptic
1605	31.3555	36.7698	31.3555	7.6414	6.5162	7.6414	26.4703	23.8724	30.5411	0.432	Elliptic
7620	18.166	36.7698	18.166	13.1895	6.5162	13.1895	45.6882	30.2806	30.3976	0.7488	Elliptic
220	36.7698	24.1575	18.166	6.5162	9.9182	13.1895	40.8802	27.5335	75.5099	0.7392	Elliptic
7611	18.166	36.7698	24.1575	13.1895	6.5162	9.9182	40.8778	27.5370	15.9141	0.7391	Elliptic
4381	24.1575	18.166	36.7698	9.9182	13.1895	6.5162	40.8801	27.5337	-44.8942	0.7392	Elliptic
8000	18.166	18.166	18.166	13.1895	13.1895	13.1895	45.6897	45.6897	0	0	Circular

4.8 Minimum to Maximum Value of Variation in Percentage Degradation in Phase-A, B and C

The Current Park's vector data pattern for the simulation combination no. '220','7611, and '4381' (refer Table 3 and Table 4), which is simulating healthy state viz. minimum –zero-percentage (0%) , '50%' of percentage degradation and maximum of 95% of percentage degradation of stator groundwall insulation degradation in 'phase-a', 'phase-b' and in 'phase-c' respectively is illustrated by Figure 12.
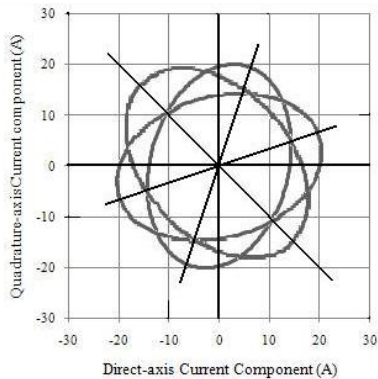

Figure 12. Current Park's Vector Pattern to Simulate Minimum to Maximum State of Stator Groundwall Insulation Degradation in Phase-A, B and C

The similar order of variation in the state of degradation of groundwall stator insulation in respective phases viz. a, b and c, leads to the same kind of deformation of Current Park's vector data pattern from circular form into an elliptical form with the same variation in the length of major –and in the minor-axes as shown in Figure 12.

5. DISCUSSION OF RESULTS

In case of equal percentage degradation in all the three phases of stator winding as shown in Figure 5; the Current Park's vector data patterns are in circular form with centre at origin and of eccentricity approximately close to zero. The length of major (M_a) and minor axis (M_b) of circular data pattern increases from '25.4012' A. to '45.6897' A. The variation is observed with respect to reference circular current vector pattern as shown in Figure 4. The change in the angular phase-shift displacement (θ°) is marginal and approximately equal to 0° with respect to positive x-axis of 'dq' coordinate plane.

As shown in Figure 6; the presence of some finite percentage of degradation of stator groundwall insulation in 'phase-c' introduce the change in the shape of Current Parks vector pattern from circular to elliptical form. The deformation in an elliptical form changes with the variation in percentage degradation in phase-c. The observed variation in the length of major axis (25.9299 A. to 37.9827 A.) is significant but in minor-axis (22.5723 A. to 22.5752 A.) is marginal with respect to reference circular current pattern as shown in Figure 4. The change in the percentage degradation of stator groundwall insulation in 'phase-c' from 25%

to maximum value of 95% leads to an increase in the deformation in elliptical pattern with the rise in the observed value of eccentricity (0.4921 to 0.8042) towards unity. The phase-shift angular displacement (θ°) oscillates approximately at around 'θ = +60°' with respect to positive x- axis with the change in the percentage degradation between 5% viz. reasonably healthy state and maximum- 95% viz. worst case of stator groundwall insulation degradation in phase-c.

The changes observed in the deformation of an elliptical pattern with the variation in the percentage degradation in 'phase-b' are exactly the same like in 'phase-c'. However, As shown in Figure 7; The phase-shift angular displacement (θ°) oscillates approximately at around 'θ = - 60°' with respect to positive x-axis with the change in the percentage degradation between 5% viz. reasonably healthy state and maximum- 95% viz. worst case of stator groundwall insulation degradation in phase-b. The changes observed in the deformation of an elliptical pattern with the variation in percentage degradation in 'phase-a' are exactly the same like in 'phase-c' and phase-'b'. However, As shown in Figure 8; The phase-shift angular displacement (θ°) remain constant at θ = 180° with respect to positive x-axis due to change in the percentage degradation between '5%' viz. reasonably healthy state and maximum- '95%' viz. worst case of stator groundwall insulation degradation in phase-a.

As shown in Figure 9; the presence of some finite percentage of degradation of stator groundwall insulation in 'phase-b' and 'phase-c' introduce the change in the shape of Current Park's vector pattern from circular to elliptical form. The deformation in an elliptical form changes with the variation in percentage degradation in 'phase-c' and 'phase-b'. The observed variations in the length of major axis (24.3976 A. to 45.6897A) and in minor-axis (23.1811A. to 30.2785A.) are both significant with respect to reference circular current vector pattern as shown in Figure 4. The change in the percentage degradation of stator groundwall insulation in 'phase-b' and 'phase-c' from 10% to maximum value of 95% leads to an increase in the deformation in elliptical pattern with the rise in the observed value of eccentricity (0.3118 to 0.7489) towards unity. The phase-shift angular displacement (θ°) remain constant at 'θ = -90°' with respect to positive x-axis of dq-coordinate plane. It is not affected on account of change in the percentage degradation between 5% viz. reasonably healthy state and maximum- 95% viz. worst case of stator groundwall insulation degradation in 'phase-b' and 'phase-c'.

The changes observed in the deformation of an elliptical pattern with the variation in the percentage degradation in 'phase-a' and 'phase-b' are exactly the same like in 'phase-b' and 'phase-c'. However, As shown in Figure 10; The phase-shift angular displacement (θ°) oscillates approximately at around 'θ = -30°' with respect to positive x-axis of dq-coordinate plane on account of change in the percentage degradation between 5% viz. reasonably healthy state and maximum- 95% viz. worst case of stator groundwall insulation degradation in 'phase-a' and 'phase-b'. The changes observed in the deformation of an elliptical pattern with the variation in percentage degradation in 'phase-a' and 'phase-c' are exactly the same like in 'phase-a' and 'phase-b'. However, As shown in Figure 11; The phase-shift angular displacement (θ°) oscillates approximately at around 'θ = +30°' with respect to positive x-axis of dq-coordinate plane on account of change in the percentage degradation between 5% viz. reasonably healthy state and maximum- 95% viz. worst case of

stator groundwall insulation degradation in 'phase-a' and 'phase-c'.

As shown in Figure 12; one of the Current Park's vector pattern which is simulating healthy state viz. minimum –zero-percentage (0%) , '50%' of percentage degradation and maximum of '95%' of percentage degradation of stator groundwall insulation degradation in phase 'a', phase-b and in phase-c respectively is in an elliptical form with centre at origin and of eccentricity equal to 0.7392. The length of major (M_a) is 40.88 A; and of minor axis (M_b) is 27.53 A. The angular phase-shift displacement (θ) is 75° approximately in anti-clockwise sense with respect to positive x-axis. The rise in the length of major (M_a) is 81.1% and of minor axis (M_b) is 21.96 % with respect to reference circular current vector pattern as shown in Figure 4. The similar order of variation in the state of degradation of groundwall stator insulation in respective phases viz. a, b and c, leads to the same kind of deformation of Current Park's vector data pattern from circular form (Є=0) into an elliptical form (Є=0.7392) with the same variation in the length of major –and in the minor-axes as shown in Figure 12. However, the phase-shift angular displacement (θ°) changes accordingly from θ = 0 ° to θ = +75°, θ = +15°, and θ = -45°, approximate value with respect to positive x-axis of dq-coordinate axes.

6. CONCLUSION

The computer –aided evaluation of percentage degradation of stator groundwall insulation of respective phases based on Park's Current transformation model provide the stator current data patterns over a large scale. Under practical circumstances it is very difficult to obtain the large set of stator current data patterns from the point of view of realization of different state of percentage degradation of stator groundwall insulation. The availability of large set of stator current data patterns emphasizes the need towards the development of the optimal design and efficient performance of artificial neural network classifier. The generated stator current data patterns can be further applied to any suitable artificial neural network (ANN) classifiers for the AI-based fault diagnosis process model to detect the degradation of stator groundwall insulation.

7. REFERENCES

[1] H. Nejjari and M. H. Benbouzid, "Monitoring and diagnosis of induction motor faults using current parks vector approach," IEEE Trans. Ind. Applicat., vol.36, no.3, May/June 2000, pp. 730-735.

[2] G. M. Joksimovic and J. Penman, "The detection of inter-turn short circuits in the stator windings of operating motors," IEEE Trans. Ind. Elect., vol.47, no.5, October 2000, pp. 1078-1084.

[3] G. B. Kliman, W. J. Premerlani, R. A. Koegland D. Hoeweler, " A new approach to on line turn fault detection in AC motors," in *Conf. Rec.* IEEE –IAS Annu. Meeting, San Diego, CA, 1996, pp. 687-693

[4] Sergio M. A. Cruz and A. J. Marques Cardoso, "Stator winding fault diagnosis in three-phase synchronous and asynchronous motors by the extended parks vector approach," IEEE *Trans. Ind. Applicat.,* vol.37, no.5, Sept./Oct. 2001, pp. 1227-1233.

[5] S. Nandi and H. A. Toliyat, " Fault diagnosis of electrical machines-A review," in Proc. IEEE Int. Electric Machines and Drives Conf. Seattle.WA, USA, May 9-12 ,1999, pp. 219-221.

[6] G. B. Kliman, W.J. Premerlani, B.Yazici, and R. A. Koegl, "Recent developments in on-line motor diagnostics," *Proc. Int. conf. Electrical Machines,* vol.1, Istanbul, Turkey, Sept.2-4, 1998, pp. 471-475.

[7] A. J. M. Cardoso et. al., "Inter turn stator winding fault diagnosis in three phase induction motors, by Park's vector approach," IEEE *Trans. Energy Conversion,* vol.14, no. 3, Sept.1999, pp. 595-598.

[8] A. J. M. Cardoso et al., "Computer aided detection of air gap eccentricity in operating three phase induction motors by Park's vector approach," IEEE *Trans. Ind. Applicat.,* vol.29, Sept. /Oct. 1993, pp. 897-901.

[9] F. C. Trutt et al., "Detection of AC machine winding deterioration using electrically excited vibrations," IEEE *Trans. Ind. Applicat.,* vol.17, no.1, 2001

[10] N. Arthur and J. Penman, "Induction machine conditioning monitoring with higher order spectra," IEEE *Trans. Ind. Elect.,* vol.47, no.5, Oct. 2000, pp. 1031-1041.

[11] F. Filippetti, G. Franceschini, C. Tassoni, and Peter Vas, "Recent developments of induction motor drives fault diagnosis using AI techniques," IEEE *Trans. Trans. Ind. Elect.,* vol.47, no.5, Oct. 2000, pp. 994-1004.